Ezrin-mediated apical integrity is required for intestinal homeostasis

Jessica B. Casaletto, Ichiko Saotome, Marcello Curto, and Andrea I. McClatchey[1]

Massachusetts General Hospital Center for Cancer Research and Department of Pathology, Harvard Medical School, Charlestown, MA 02129

Edited by Joan S. Brugge, Harvard Medical School, Boston, MA, and approved June 14, 2011 (received for review March 1, 2011)

Individual cell types are defined by architecturally and functionally specialized cortical domains. The Ezrin, Radixin, and Moesin (ERM) proteins play a major role in organizing cortical domains by assembling membrane protein complexes and linking them to the cortical actin cytoskeleton. Many studies have focused on the individual roles of the ERM proteins in stabilizing the membrane–cytoskeleton interface, controlling the distribution and function of apical membrane complexes, regulating the small GTPase Rho, or establishing cell–cell junctions. We previously found that deletion of the mouse *Ezrin* gene yields severe defects in apical integrity throughout the developing intestinal epithelium, resulting in incomplete villus morphogenesis and neonatal death. However, the molecular function of Ezrin in building the apical surface of the intestinal epithelium was not clear. By deleting *Ezrin* in the adult mouse intestinal epithelium, we provide evidence that Ezrin performs multiple molecular functions that collaborate to build the functional apical surface of the intestinal epithelium in vivo. The loss of Ezrin-mediated apical integrity in the adult intestine yields severe morphological consequences during intestinal homeostasis, including defects in cell geometry, extrusion, junctional remodeling, and spindle orientation. Surprisingly, deletion of Ezrin either before or after villus morphogenesis yields villus fusion, revealing a previously unrecognized step in intestinal homeostasis. Our studies indicate that the function of Ezrin in building and maintaining the apical domain is essential not only for intestinal morphogenesis but also for homeostasis in the mature intestine.

actomyosin contractility | planar cell polarity | colon | Merlin

The vast array of forms and functions exhibited by different cell types is made possible by the organization of specialized domains within the cell cortex. The assembly of such domains involves the coordination of processes occurring at the plasma membrane with those in the underlying cytoskeleton. Central to this coordination is the formation of protein complexes on the cytoplasmic side of the plasma membrane that localize membrane proteins, control their abundance and activity, and link them to the cortical cytoskeleton, thereby serving both regulatory and architectural functions.

The ERM proteins (ERMs) can assemble multiprotein complexes at the membrane–cytoskeleton interface and play a key role in organizing the apical domain of polarized epithelial cells (1, 2). These proteins harbor a trilobed N-terminal FERM (*F*our-point-one-*ERM*) domain that provides multiple protein-binding interfaces and mediates plasma membrane association and a C-terminal domain that can associate directly with F-actin (3, 4). The FERM domain can bind directly to any of several transmembrane proteins or to PDZ domain-containing adapters such as NHERF1 (Na^+/H^+ exchanger regulatory factor 1), which, in turn, can associate with additional transmembrane proteins (1, 5, 6). Given this structure, the ERMs can potentially link multiple proteins to the actin cytoskeleton. As such, they are thought to both stabilize the cortical actin cytoskeleton and control the assembly, distribution, and activity of certain membrane-associated complexes, although these functions have been largely studied independently. For example, studies in flies and cultured mammalian cells reveal a key role for the ERMs in stabilizing the membrane–cytoskeleton interface during bleb retraction, mitotic cell rounding, and the establishment and maintenance of apical cell–cell junctions (7–10). Other studies have documented a role for ERMs in assembling apical membrane complexes (11–14). Studies in the fly indicate that yet another key function of the single *Drosophila* ERM protein, Moesin, is to negatively regulate the small GTPase Rho1 (15). Therefore, the ERMs may do at least three things, perhaps simultaneously and in coordination: (*i*) stabilize the membrane–cytoskeleton interface, (*ii*) regulate the formation of apical membrane complexes, and (*iii*) control Rho1 (RhoA in mammals, hereafter referred to as "Rho") activity.

The specialized apical domains of thousands of individual intestinal epithelial cells work together to carry out the absorptive function of the intestine while providing a strong, flexible network that can withstand and respond to mechanical stress during constant homeostatic cell movement. This apical brush border (BB) domain features a dense mat of microvilli that increase the absorptive surface area of the gut and are anchored in a thick, contractile cytoskeletal platform known as the terminal web. The terminal web is integrated with the circumferential apical junctional region (AJR), allowing mechanical coupling among cells across the epithelium.

Recent studies from our laboratory and others have revealed a key role for ERM function in building the apical domain of intestinal epithelial cells in vivo (16–18). Loss of Ezrin, the only ERM expressed in the mouse intestinal epithelium, or of the single ERM ortholog (ERM-1) in *Caenorhabditis elegans*, yields remarkably similar defects in apical integrity throughout the developing intestinal epithelium. In the absence of Ezrin/ERM-1, intestinal epithelial cells establish apical-basal polarity and form microvilli, but exhibit defects in the morphology of the apical domain, particularly in the terminal web and associated junctions (16, 18). In the developing mouse intestine, this results in the incomplete expansion of secondary lumina that would normally segregate individual villi (16). *Ezrin*-null mice fail to thrive and do not survive past weaning; whether this is due to architectural defects in villus morphogenesis, aberrant function of apical transporters, or both is not known. Moreover, the molecular function of Ezrin in building the apical surface of the intestinal epithelium is not clear. By deleting *Ezrin* in the adult mouse intestine, we demonstrate that (*i*) Ezrin performs multiple molecular functions in vivo and (*ii*) the function of Ezrin in building and maintaining the apical domain is essential not only for morphogenesis but also for homeostasis in the mature intestine.

Author contributions: J.B.C., I.S., M.C., and A.I.M. designed research; J.B.C., I.S., and M.C. performed research; J.B.C., I.S., and A.I.M. analyzed data; and J.B.C. and A.I.M. wrote the paper.

The authors declare no conflict of interest.

This article is a PNAS Direct Submission.

[1]To whom correspondence should be addressed. E-mail: mcclatch@helix.mgh.harvard.edu.

This article contains supporting information online at www.pnas.org/lookup/suppl/doi:10.1073/pnas.1103418108/-/DCSupplemental.

Results

Ezrin Is Required Cell-Autonomously for Apical Morphogenesis in the Adult Mouse Intestine. Constitutional *Ezrin* null ($Ez^{-/-}$) mice die as neonates with intestinal defects but without other detectable abnormalities (16). To confirm that the phenotype of $Ez^{-/-}$ neonates was due to a cell-autonomous requirement for Ezrin in the intestinal epithelium, we generated *Villin(Vil)-Cre;*$Ez^{lox/lox}$ mice in which *Ezrin* is deleted specifically in intestinal epithelial cells during development (19). We found that *Vil-Cre;*$Ez^{lox/lox}$ mice are phenotypically identical to $Ez^{-/-}$ mice, exhibiting the same defects in apical integrity, villus morphogenesis, and neonatal death (Fig. S1) (16).

To bypass the neonatal lethality of $Ez^{-/-}$ and *Vil-Cre;*$Ez^{lox/lox}$ mice and examine the requirement for Ezrin function in the adult intestine after villus morphogenesis, we crossed $Ez^{lox/lox}$ mice (16) to transgenic *Vil-Cre-*ER^{T2} mice in which Cre activity can be induced via tamoxifen injection (19). Tamoxifen treatment of adult *Vil-Cre-*ER^{T2}*;*$Ez^{lox/lox}$ mice led to recombination of the *Ez* allele and complete loss of Ezrin throughout the colonic and small intestinal epithelia (Fig. S2). Tamoxifen-treated mice were viable but exhibited severe defects in apical integrity that were nearly identical to that seen in $Ez^{-/-}$ or *Vil-Cre;*$Ez^{lox/lox}$ neonates in which *Ezrin* was deleted before villus morphogenesis (Fig. S1) (16). For example, instead of the highly organized wild-type BB composed of a compact, cytoskeletal terminal web and uniformly sized and oriented microvilli (Fig. 1 *A* and *C*), deletion of *Ezrin* in the adult intestine yielded a distended terminal web and nonuniform, misoriented microvilli (Fig. 1 *B* and *D* and Fig. S3). In fact, $Ez^{-/-}$ microvilli exhibit a spectrum of morphologies—from distinct, individual units [i.e., Fig. 1 *E* and *F* and *D* (top)] to a more "weblike" morphology [i.e., Fig. 1*D* (bottom)] to a gross herniation of the entire apical membrane (i.e., Fig. 1 *E* and *F*). We interpret this to reflect a requirement for Ezrin in tethering the membrane to the cortical cytoskeleton at the base of each microvillus and/or organizing the terminal web from which they protrude. In fact, in contrast to the continuous apical accumulation of actin in control epithelia (Fig. 1*G*), apical actin is often ragged and discontinuous in the absence of Ezrin (Fig. 1*H*), further supporting an important role for Ezrin in stabilizing the membrane–cortical cytoskeleton in vivo. Notably, these defects were seen throughout the small intestine and in the colon, which was not examined in our earlier study (16).

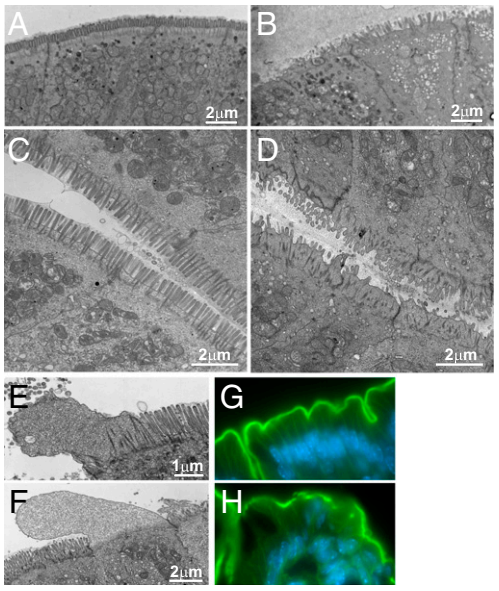

Fig. 1. Apical defects in the adult $Ez^{-/-}$ intestine. (*A–D*) Transmission EM of intestinal epithelia from tamoxifen-treated $Ez^{lox/lox}$ (*A* and *C*) and *Vil-Cre-*ER^{T2}*;*$Ez^{lox/lox}$ (*B* and *D*) mice. Control colonic (*A*) and small intestinal (*C*) epithelia maintain a highly organized BB featuring densely packed, uniform microvilli with actin rootlets embedded in a compact terminal web. $Ez^{-/-}$ microvilli in colonic (*B*) and small intestinal epithelia (*D*) are nonuniform, misoriented, and extend from a thickened and disorganized terminal web; actin rootlets are disorganized or absent. (*A* and *B*) 2,900× magnification. (*C* and *D*) 11,000× magnification. (*E* and *F*) Large blebs of membrane no longer attached to the cytoskeleton are frequently found throughout the $Ez^{-/-}$ intestine. (*E*) 15,000× magnification. (*F*) 7,100× magnification. (*G* and *H*) Phalloidin-stained colonic epithelia reveal the continuous apical band of actin labeling of the BB of control cells (*G*); actin is discontinuous in $Ez^{-/-}$ cells (*H*). (*G* and *H*) 600× magnification.

Loss of Ezrin Disrupts the Formation of Apical Membrane Complexes. Given that Ezrin can bind to membrane-associated receptors and adapters and is essential for apical membrane integrity, we expected that apical membrane complexes that rely on Ezrin would be disrupted in vivo. For example, recent studies indicate that fly Moesin, Sip1 (the *Drosophila* ortholog of NHERF1), and Slik (a kinase necessary for Moesin phosphorylation and activation in the fly) form an interdependent apical complex (20). A major advantage of deleting *Ezrin* in the adult is that, in contrast to $Ez^{-/-}$ neonates, the adult intestine yields enough tissue for biochemical analysis. Indeed, biochemical fractionation of BB components revealed that the levels of Slk (the mammalian homolog of Slik) are markedly reduced in BBs isolated from the $Ez^{-/-}$ intestine (Fig. 2*A* and Fig. S3*C*). Similarly, NHERF1 fails to localize apically in the adult $Ez^{-/-}$ intestine, as in the neonate (16), and is not present in isolated BBs (Fig. 2 *A–C*). Notably, the total levels of NHERF1 are also reduced in the $Ez^{-/-}$ intestinal epithelium, suggesting that NHERF1 stability may depend on its localization and/or interaction with Ezrin. This is consistent with the finding that loss of Moesin decreases the overall abundance of Sip1 in the fly (20). NHERF1 is known to associate with and regulate the ion transporters NHE3 and CFTR in the intestine (21), suggesting that they may be misregulated in the absence of Ezrin. Misregulation of these transporters in mouse models causes fat malabsorption (22). Indeed, fecal analysis revealed the presence of excess fats in feces from $Ez^{-/-}$ intestines (*Materials and Methods*). Together these data indicate that Ezrin is required for the assembly and function of BB membrane complexes in vivo.

Increased Rho Activity in the Absence of Ezrin. A key function of *Drosophila* Moesin is to negatively regulate Rho (15). Moreover, in cultured mammalian kidney cells, expression of a dominant-

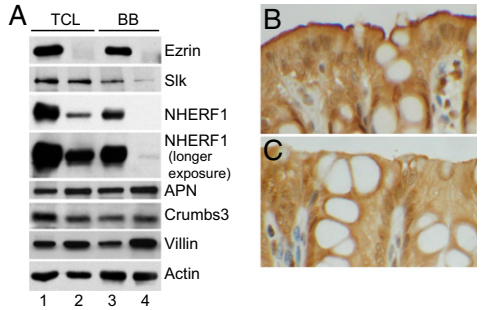

Fig. 2. Loss of Ezrin disrupts the formation of apical membrane complexes. (*A*) BBs were isolated from control (lanes 1 and 3) and $Ez^{-/-}$ (lanes 2 and 4) small intestines. Total cell lysate (TCL) and BB fractions were solubilized in the presence of 1% SDS. Villin served as a positive control for the BB fraction and aminopeptidase N (APN), and Crumbs3 served as controls for apical membrane proteins. Note the specific loss of NHERF1 and Slk in $Ez^{-/-}$ BBs. (*B* and *C*) NHERF1 is apically concentrated in colonic epithelia from tamoxifen-treated $Ez^{lox/lox}$ (control, *B*), but not *Vil-Cre-*ER^{T2}*;*$Ez^{lox/lox}$ ($Ez^{-/-}$, *C*) mice.

negative form of Ezrin increased Rho activity (15). It is not known, however, whether Rho inhibition is a general property of mammalian ERMs, as no suitable model for testing this hypothesis in vivo was previously available. Therefore, we measured Rho activity in control and $Ez^{-/-}$ epithelia. Despite similar total levels of Rho, levels of active Rho were increased in both $Ez^{-/-}$ colonic and small intestinal epithelia (Fig. 3*A* and Fig. S4*A*). This was accompanied by an increase in phosphorylation of myosin light chain 2 (MLC2), a target of Rho and a mediator of actomyosin contractility (Fig. 3*B* and Fig. S4*B*), and by the altered distribution of phosphorylated MLC2 (pMLC2). In isolated control cells, pMLC2 was concentrated at the compact apical surface with an additional diffuse localization throughout the cell (Fig. 3*C*). In contrast, pMLC2 was markedly enriched in the thickened apical region in $Ez^{-/-}$ cells and exhibited a punctate distribution throughout the cell (Fig. 3*D*), reminiscent of the contractile myosin aggregates seen in *Drosophila* S2 cells that lack Moesin (9).

Morphogenetic Consequences of Ezrin Deficiency in the Adult Intestine. We expected that defects in Rho regulation and in the integrity of the apical domain would affect the dynamic architecture of the $Ez^{-/-}$ intestinal epithelium. Indeed, $Ez^{-/-}$ cells throughout the intestine exhibit a morphology that is distinct from their wild-type counterparts. Whereas wild-type cells have a wider apical surface relative to the middle or basal region, $Ez^{-/-}$ cells are uniformly narrow. This is particularly pronounced in the colon where wild-type cells exhibit markedly expanded apical membranes as they execute a 90 degree turn at the transition from the crypt to the colon surface (Fig. 4*A*). In contrast, $Ez^{-/-}$ cells maintain narrow apical surfaces such that nearly twice as many cells accomplish this transition (Fig. 4 *B* and *C*). This is consistent with the possibility that the apical surface of $Ez^{-/-}$ cells cannot expand due to excess Rho-mediated actomyosin contractility. Similar differences were seen at the crypt–villus junction of the small intestine.

The adult intestinal epithelium is in a constant state of movement, with newborn cells continuously migrating from the crypts to villus tips or the colonic surface where they are extruded into the intestinal lumen (23). Rho-dependent actomyosin contractility is known to be critical for epithelial cell extrusion (24). In fact, excess apical Rho activity has been linked to a failure of apical extrusion in cultured cells (25). Therefore, we suspected that there might be a defect in the extrusion of cells

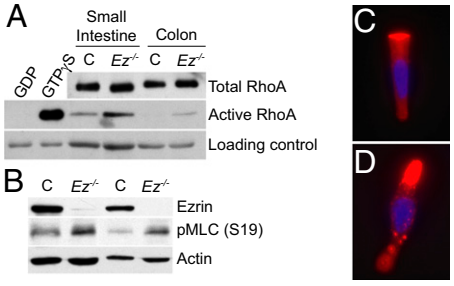

Fig. 3. Increased Rho activity in $Ez^{-/-}$ intestinal epithelial cells. (*A–D*) Cells from vehicle (C) or tamoxifen-treated ($Ez^{-/-}$) *Vil-Cre-ER*^{T2};*Ez*$^{lox/lox}$ mice were analyzed. (*A*) Cell lysates were incubated with GST-Rhotekin beads. Bound proteins (active) and total cell lysates (total) were examined. Preincubation with GDP or GTPγS served as negative and positive controls, respectively. The amount of beads in each reaction served as a loading control for each pair. (*B*) Small intestinal epithelial cell lysates from two pairs of C and $Ez^{-/-}$ mice reveal increased levels of pMLC in $Ez^{-/-}$ cells. (*C* and *D*) Control (*C*) or $Ez^{-/-}$ (*D*) small intestinal epithelial cells were immunostained with antibodies against pMLC (Ser19) (red) and DAPI (blue). In $Ez^{-/-}$ cells, pMLC is enriched in the thickened apical region and present in punctate aggregates (*D*). (*C* and *D*) 600× magnification.

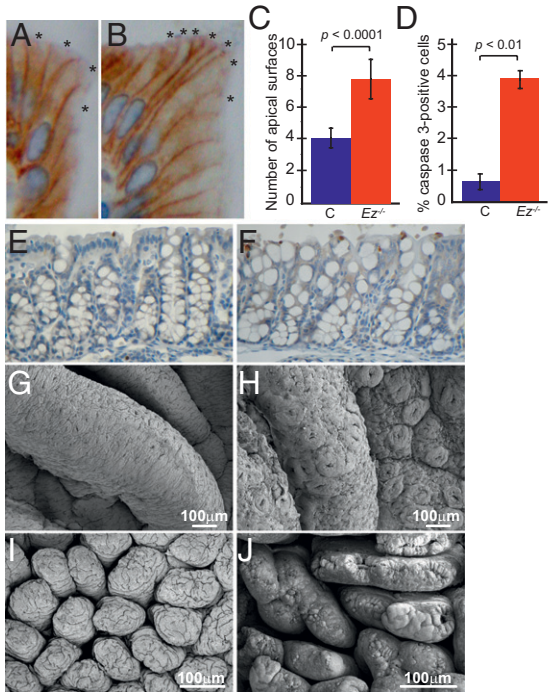

Fig. 4. Morphogenetic consequences of Ezrin loss in the adult intestine. (*A–C*) Altered shape of $Ez^{-/-}$ epithelial cells. (*A* and *B*) β-Catenin staining in colonic epithelia from tamoxifen-treated $Ez^{lox/lox}$ (control, *A*) and *Vil-Cre-ER*^{T2};*Ez*$^{lox/lox}$ ($Ez^{-/-}$, *B*) mice reveals expanded apical surfaces of control cells as they transition from the crypt to the colonic surface (*A*) in contrast to the nearly uniformly narrow $Ez^{-/-}$ cells (*B*). An asterisk marks the apical surfaces that compose this transition and provides an example of the quantitation shown in *C*. (*A* and *B*) 600× magnification. (*C*) The number of apical surfaces per transition in control (C) (4.0 ± 0.6) and $Ez^{-/-}$ (7.6 ± 1.3) mice were determined using two mice of each genotype ($P < 0.0001$). (*D–F*) Decreased extrusion of apoptotic cells in $Ez^{-/-}$ epithelia. Cleaved caspase-3 staining of control (*E*) and $Ez^{-/-}$ (*F*) epithelia reveals a sixfold increase in positive cells at the colonic surface in the absence of Ezrin (control, 0.64% ± 0.25; $Ez^{-/-}$, 3.8% ± 0.28; $P < 0.01$). A minimum of 1,000 epithelial cells per colon were counted using two mice of each genotype. (*G* and *H*) SEM across the luminal surface of the colon. Apical defects result in a rough, nonuniform appearance of the $Ez^{-/-}$ colon (*H*) compared with the smooth, uniform surface of the control (*G*). (*G* and *H*) 130× magnification. (*I* and *J*) SEM across the luminal surface of the small intestinal epithelium from control (*I*) and $Ez^{-/-}$ (*J*) mice. Single-villus units cover the control small intestine, whereas $Ez^{-/-}$ intestines contain villus structures composed of two or more individual villi fused together. (*I* and *J*) 250× magnification.

from $Ez^{-/-}$ intestines. Normally, cells are extruded before visible signs of apoptosis. Indeed, we found a sixfold increase in the percentage of cleaved caspase-3–positive cells at the surface of the $Ez^{-/-}$ colonic epithelium (control = 0.64%; $Ez^{-/-}$= 3.8%) (Fig. 4 *D–F*), suggesting that $Ez^{-/-}$ cells receive the extrusion signal but are not physically removed in a timely manner (24). The altered apical morphology of cells at the crypt surface, together with defects in cell extrusion, yields a prominent difference in the contour of the colonic surface epithelium as highlighted by scanning electron microscopy (SEM). The surface of the $Ez^{-/-}$ colon is studded with donut-shaped accumulations of cells surrounding the mouth of each crypt (Fig. 4*H*), in contrast to the smooth, uniform surface of control tissue (Fig. 4*G*).

It is not surprising that deletion of Ezrin from the adult small intestine and colon led to apical defects similar to those of $Ez^{-/-}$ neonates (16). However, the prominent villus fusion phenotype of $Ez^{-/-}$ and *Vil-Cre*;$Ez^{lox/lox}$ mice arises in the embryo due to defects in the earliest stages of villus formation (16); therefore, we did not anticipate that deletion of *Ezrin* from the mature

intestine *after* villus morphogenesis would also lead to the fusion of villi across the small intestine, a defect that is readily visualized by SEM (Fig. 4*J*). Instead of individual units of architecture (Fig. 4*I* and Fig. S5*A*), $Ez^{-/-}$ villi formed amalgamated structures composed of two or more villi that were fused to form a single architectural unit (Fig. 4*J* and Fig. S5*B*). The extent of fusion between $Ez^{-/-}$ villi increased with time after *Ezrin* deletion until the villi were fused along their entire length, arguing that villus fusion occurs during the continuous repopulation of the villus with cells from the crypt.

Ezrin Stabilizes the AJR in the Mammalian Intestinal Epithelium. The remarkably similar phenotypes of $Ez^{-/-}$ neonates and adults suggest that villus fusion results from the same underlying defect in development and homeostasis. During development, villus morphogenesis is driven in part by the de novo formation and expansion of secondary lumina throughout the stratified epithelium that originally lines the gut tube, converting it into a columnar monolayer and driving the segregation of individual villi (26, 27). A key step in this process is the progressive conversion of cell junctions into a new apical surface. In the absence of Ezrin, secondary lumina form but often fail to expand, yielding incomplete segregation of villi (16). In the adult, the epithelium is already a columnar monolayer; it is the turnover of this monolayer that requires precise and dynamic regulation of cell junctions. The intricate cell rearrangements that occur as cells migrate from crypt to villus in the adult have not been well-mapped; however, cells from each crypt contribute to more than one villus, and some must segregate at the crypt–villus transition. Thus, villus fusion in the adult likely results from defects in junctional remodeling during this transition. Indeed, recent studies have reported roles for the ERMs in stabilizing and remodeling the AJR in worms, flies, and mammals (10, 16, 18, 28). This would also be consistent with the well-documented role for Rho in expanding and stabilizing apical junctions in mammalian cells (29–31). To determine whether Ezrin stabilizes the intestinal AJR, we examined the wild-type and $Ez^{-/-}$ AJR morphologically and biochemically. Transmission electron microscopy revealed that, instead of the compact AJR that contains parallel, closely apposed membranes in wild-type epithelia (Fig. 5*A*), deletion of *Ezrin* led to elongated and sinuous junctions that often contained obvious gaps between points of close apposition (Fig. 5*B*).

Biochemical fractionation provided additional evidence that the AJR is altered in the absence of Ezrin. The solubilities of the core adherens junction (AJ) components E-cadherin, β-catenin, and α-catenin were dramatically increased in $Ez^{-/-}$ BBs (Fig. 5*C*). We also found that AJ components were associated with higher-molecular-weight complexes in the absence of Ezrin. Sucrose gradient centrifugation of lysates from control and $Ez^{-/-}$ intestines revealed that AJ components in control cells sedimented mainly in fractions 3–6, although significant levels of AJ proteins were also present in higher-molecular-weight fractions in $Ez^{-/-}$ cells (Fig. S6). Immunoprecipitation of E-cadherin from these fractions revealed the association of α-catenin and β-catenin, suggesting that the core AJ complex associates with different proteins in the presence and absence of Ezrin (Fig. 5*D*).

Altered Spindle Orientation in the Absence of Ezrin. Our biochemical data fit well with the growing appreciation that the AJR is a dynamic and heterogeneous structure (28, 32, 33). For example, recent studies suggest that the AJR contains cadherin complexes that are either freely moving or part of actin-associated clusters that are embedded in a contractile cortical cytoskeleton (34). Moreover, within the AJR, AJ proteins can exhibit asymmetric (planar polarized) distributions that drive polarized cell rearrangements, perhaps reflecting underlying differences in the distribution and/or composition of cadherin clusters (35–38).

Planar polarity has not been studied in the intestine, but the fact that cells constitutively migrate from crypt to villus suggests

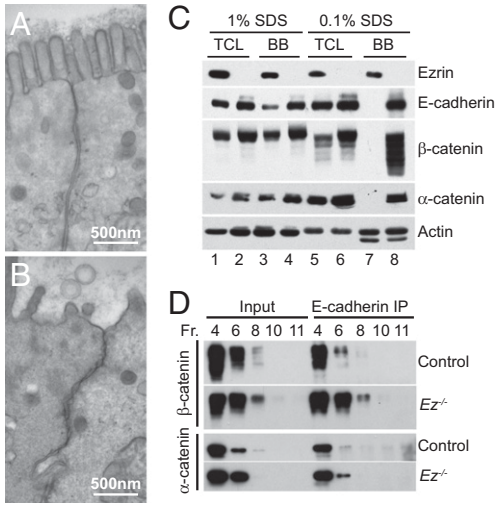

Fig. 5. Defects in the AJR of $Ez^{-/-}$ intestinal epithelia. (*A* and *B*) Transmission EM of colonic epithelia from tamoxifen-treated $Ez^{lox/lox}$ (control, *A*) and *Vil-Cre-ER*^{T2}*;Ez*$^{lox/lox}$ ($Ez^{-/-}$, *B*) mice reveals defective AJR architecture in the absence of Ezrin. (*A* and *B*) 11,000× magnification. (*C*) Increased solubility of AJ components in the $Ez^{-/-}$ BB. AJ components in the total cell lysate (TCL) and BB fractions of control (lanes 1, 3, 5, and 7) and $Ez^{-/-}$ (lanes 2, 4, 6, and 8) small intestinal epithelia were solubilized in the presence of 1% or 0.1% SDS. Note the increased solubility in $Ez^{-/-}$ BBs. The solubilities of the tight junction proteins ZO-1 and occludin were also increased (Fig. S7). (*D*) Co-immunoprecipitation of β-catenin and α-catenin with E-cadherin in the indicated sucrose gradient fractions (Fig. S6) reveals the presence of higher-molecular-weight AJ complexes in $Ez^{-/-}$ intestines.

that they know their orientation relative to this axis. Given the essential role of Ezrin in building the apical cortex of intestinal epithelial cells, together with the altered biochemical properties of AJ complexes in the absence of Ezrin, we suspected that Ezrin might be required for planar orientation in the intestinal epithelium. A signature of planar polarity in other tissues is spindle orientation (39–41). Spindles in transit amplifying cells of the crypts are known to align parallel to the apical surface, but it is not clear whether they are planar-polarized (parallel to the apical surface *and* specifically oriented relative to the crypt–villus axis). Indeed, we found that most spindles in control crypts were aligned parallel to the apical surface as has been described (42, 43); we also found that they were predominantly oriented along the crypt–villus axis, indicating that they are planar-polarized (Fig. 6 *A* and *C* and Movie S1). In contrast, spindles in $Ez^{-/-}$ crypts, although still parallel to the apical surface, exhibited a near random orientation relative to the crypt–villus axis (Fig. 6 *B* and *C* and Movie S2). Confocal imaging and 3D reconstruction allowed for quantitation of spindle orientation. Thus, whereas 91% of control spindles were aligned within 30 degrees of the crypt–villus axis, only 67% of spindles in $Ez^{-/-}$ cells were similarly aligned (Fig. 6*C*). These data suggest that Ezrin-dependent organization of the apical cortex is required for planar-polarized spindle orientation in the intestinal epithelium.

Discussion

By bringing together multiple proteins at the membrane and linking them to the cytoskeleton, the ERMs seem designed to simultaneously coordinate several activities at the cell cortex. Studies of the ERMs across species have independently focused on their roles in stabilizing the membrane–cytoskeleton interface, regulating the small GTPase Rho, controlling membrane receptors, or stabilizing the AJR. Here, we provide evidence that the ERMs carry out all of these functions in the same tissue in vivo, supporting the notion that individual ERM molecules can simultaneously coordinate multiple activities. Moreover, we extend

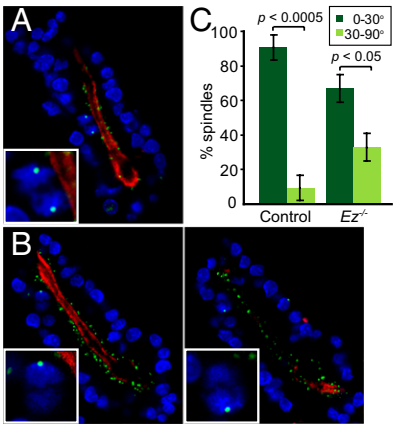

Fig. 6. Altered spindle orientation in the absence of Ezrin. (*A* and *B*) Immunostaining with anti-pericentrin antibodies (green), phalloidin (red, marks the crypt–villus axis), and DAPI (blue) reveals spindle orientation in small intestinal crypts from tamoxifen-treated $Ez^{lox/lox}$ (control, *A*) and *Vil-Cre-ER*^{T2};$Ez^{lox/lox}$ ($Ez^{-/-}$, *B*) mice. Representative single *z*-plane images are presented. Note that both centrosomes are found in a single *z*-plane in control crypts (*A*), whereas the two centrosomes in *B* are in distinct *z*-planes that are 4 μm apart. (*C*) Quantitation of spindle orientation carried out by confocal imaging and 3D reconstruction reveals that 91% ± 7.5% ($n = 23$; $P < 0.0005$) of spindles in control crypts were aligned within 30° of the crypt–villus axis, whereas only 67% ± 8.0% ($n = 30$; $P < 0.05$) of spindles in $Ez^{-/-}$ crypts were aligned in this manner (overall $P < 0.05$).

our previous discovery of the requirement for Ezrin in intestinal development and show that Ezrin function is also necessary for intestinal homeostasis in the adult. In fact, the phenotypic consequences of deleting *Ezrin* before villus morphogenesis (during development) *vs.* during villus maintenance (in the adult) are essentially identical, uncovering a previously unrecognized morphogenetic aspect of intestinal homeostasis. We also provide evidence that the intestinal epithelium is planar-polarized.

The ability of the ERMs to directly control both local cortical architecture and receptor distribution/activity renders them pivotal in creating cortical domains that define the functions of individual cells or tissues. Ezrin coordinates these molecular functions to build a contractile apical domain that also carries out the absorptive function of the intestinal epithelium. Conversely, the loss of apical integrity due to Ezrin deficiency reflects the concomitant loss of multiple molecular functions and profoundly impacts intestinal architecture, function, and homeostasis. On a cellular level, destabilization of the membrane–cytoskeleton interface and increased Rho-mediated actomyosin contractility likely cooperate to give rise to a BB that exhibits misoriented microvilli and is prone to herniation. Microvilli function to increase the absorptive surface area of the gut and present transporters to the intestinal lumen. Therefore, these defects may reflect the function of Ezrin both in stabilizing the membrane–cytoskeleton interface and in presenting and regulating critical transporters. Notably, recent studies indicate that microvilli can function as dynamic conveyor belts that continuously shed active enzyme-containing vesicles into the intestinal lumen, highlighting the importance of coordinating mechanically stable membrane–cytoskeleton attachment with the positioning and regulation of membrane protein complexes (44).

The intestinal epithelium is the most dynamic tissue in the adult body, replacing billions of cells every 4–5 d through an exquisitely choreographed program of cell division, migration, and extrusion (23). The interconnected BBs of intestinal epithelial cells provide a strong, flexible network that maintains the integrity of the epithelium while cells are in constant movement and under continuous mechanical stress. The apical surfaces of $Ez^{-/-}$ cells across the epithelium are narrow and do not expand at the crypt surface, consistent with the notion that they are constrained by excess Rho-mediated actomyosin contractility. Moreover, the extrusion of apoptotic cells from the colonic epithelium, which is driven by a transient relaxation of Rho-mediated contractility, is defective in the absence of Ezrin. These defects highlight the dynamic nature of Rho-mediated contractility that must govern these processes and suggest that the role of Ezrin in Rho regulation is also dynamic.

The most profound defect caused by loss of Ezrin in the adult is the development of fused villi. Surprisingly, this phenotypically mirrors the consequences of *Ezrin* deficiency in the developing intestine, a defect attributable to the failed expansion of secondary lumina that drive villus segregation specifically during development. However, careful consideration reveals that both of these defects may reflect failed segregation of cells due to defective junctional remodeling and are therefore likely to be directly related. In the adult, crypts significantly outnumber villi (23), and each crypt contributes to several surrounding villi. Therefore, the process of continuous villus repopulation must involve the segregation of adjacent cells at some point. In the $Ez^{-/-}$ intestine, adjacent cells appear unable to segregate and instead remain in contact as they ascend two different villi, resulting in villus fusion (Fig. 4*J* and Fig. S5*B*). This defect could be due to defective planar polarization of cell junctions. The segregation of adjacent cells before migration up separate villi implies that cell junctions aligned with the crypt–villus axis, but not those perpendicular to it, are programmed for segregation. Our observation that spindle orientation is planar-polarized in the wild-type but not in the $Ez^{-/-}$ intestine, together with morphological and biochemical differences in the AJR in the absence of Ezrin, support this hypothesis.

The mechanism by which Ezrin stabilizes the AJR may be indirect. Studies in *Drosophila* demonstrated that, through interaction with the membrane-tethered protein Bitesize (Btsz), Moesin organizes actin in a localized domain that is in turn required to stabilize E-cadherin (10). In *btsz* mutants, Moesin localization to the AJR is decreased and E-cadherin is not stabilized, as actin filaments fail to form a stable, continuous network that defines the boundary between the apical and junctional domains. Indeed, the elongated and disorganized appearance of cell–cell junctions in $Ez^{-/-}$ intestinal epithelia (Fig. 5*B*) could reflect the lack of a properly defined apical–junctional boundary. However, although several mammalian homologs of Btsz exist, none contain the Moesin-interacting domain (10).

Our data uncover the complex molecular requirements for Ezrin in building the apical BB and the similarly complex biological requirements for the apical BB in intestinal epithelial homeostasis. This model will be valuable for a detailed biochemical interrogation of Ezrin-containing complexes in the intestinal epithelium and for deeper analyses of individual aspects of intestinal homeostasis.

Materials and Methods

SI Materials and Methods provides further details.

Animals and Animal Procedures. $Ez^{lox/lox}$ mice (16) were crossed with tamoxifen-inducible *Vil-Cre-ER*^{T2} transgenic mice provided by Sylvie Robine (Institut Curie, Paris) (19). Tamoxifen (MP Biomedicals) was solubilized (50 mg/mL in ethanol) and diluted to 10 mg/mL in corn oil. Mice (12–18 wk of age) were injected i.p. with 100 μL tamoxifen or vehicle/day for 5 d and killed 4–5 d after cessation of treatment. For fecal analysis, feces were collected for 48 h and submitted to Idexx Laboratories for examination. Animal procedures were performed according to federal and institutional guidelines and approved by the Massachusetts General Hospital Subcommittee on Research Animal Care.

Histochemistry and Immunohistochemistry. Tissues were fixed in formalin. Sections were stained with hematoxylin and eosin or by immunohistochemistry using the following antibodies: Neomarkers (Ezrin, 3C12; Moesin, 38/87), Abcam (NHERF1, ab3452), BD Biosciences (β-catenin, 610154), and Cell Sig-

naling (cleaved caspase-3, 9661). HRP-conjugated secondary antibodies were detected using a DAB (3,3′-diaminobenzidine) kit (Vector Laboratories).

Electron Microscopy. For transmission electron microscopy (EM), small intestinal tissue was fixed in 4% glutaraldehyde and prepared and imaged as described (16). Colonic tissue was fixed in 2.5% glutaraldehyde/2.5% paraformaldehyde in 0.1 M sodium cacodylate buffer (Electron Microscopy Sciences), prepared as above, examined on a Tecnai G^2 Spirit BioTWIN electron microscope, and captured as above. For scanning EM, tissues were fixed in 2.5% glutaraldehyde, postfixed in 1% osmium tetroxide (both in 0.1 M phosphate buffer), and dehydrated. Samples were sputter-coated with 15 nm gold:palladium and examined on a Hitachi S-4800 field emission scanning electron microscope.

Rho Activity Assay. Intestines were flushed with PBS, opened, and placed in buffer [50 mM Tris·Cl (pH 7.4), 150 mM NaCl, 10 mM $MgCl_2$, 5% glycerol, 1% Triton-X 100, 0.1% SDS, and a protease/phosphatase inhibitor mixture]. Cells were scraped into buffer, lysed (10 min, ice), cleared (13,000 × *g* 5 min, 4 °C), and incubated with GST-Rhotekin-Sepharose (45 min, 4 °C). For controls, 1 mM GDP and 100 μM GTPγS were added to lysates.

BB Isolation. BBs were isolated using the method described by the Tyska laboratory (44).

Immunofluorescence. Intestinal epithelial cells (IECs) were isolated as above, washed, and fixed in 4% paraformaldehyde (PFA). Cells were blocked in 10% goat serum and incubated with anti-pMLC2 antibodies (Cell Signaling; #3675). Crypts were isolated by incubation of small intestines in 3 mM EDTA/0.5 mM DTT (90 min, ice) and mechanical fractionation in PBS. Crypts were washed, fixed in 4% PFA, blocked, permeabilized in 2% BSA/0.1% Triton-X 100, and incubated with anti-pericentrin antibodies (Abcam ab4448).

Sucrose Gradient Centrifugation and Immunoprecipitations. IECs were isolated as above, lysed in triton lysis buffer [135 mM NaCl, 50 mM Tris·Cl (pH 7.4), 1 mM EDTA, 1 mM EGTA, 1% Triton-X 100, and a protease/phosphatase inhibitor mixture], cleared (14,000 × *g*, 30 min, 4 °C), and resolved on 12 mL 5–30% wt/vol sucrose gradients (28,000 × *g*, 18 h, 4 °C). For immunoprecipitations, anti–E-cadherin antibodies (BD Biosciences; 610182) were incubated with fractions (16 h, 4 °C) and recovered on Protein A-Sepharose (GE Healthcare) (2 h, 4 °C).

Immunoblotting. IECs and BBs were lysed in RIPA buffer (16) (1 h, ice) or 1% SDS buffer [10 mM Tris·Cl (pH 7.4), 1% SDS, 50 mM NaF, 1 mM Na_3VO_4] (10 min, 100 °C) and cleared (14,000 × *g*, 30 min, 4 °C). Proteins were detected using the indicated antibodies.

ACKNOWLEDGMENTS. We thank Sylvie Robine for *Vil-Cre-ER^{T2}* mice; Ben Margolis for anti-Crumbs3 antibodies; Bill Fowle and Thomas Diefenbach for assistance with electron and confocal microscopy; and Kevin Haigis, Silvia Fre, and Matt Tyska for advice and discussion. This work was supported by National Institutes of Health Grant R01GM087558 (to A.I.M.) and a Children's Tumor Foundation Young Investigator Award (to J.B.C.).

1. McClatchey AI, Fehon RG (2009) Merlin and the ERM proteins: Regulators of receptor distribution and signaling at the cell cortex. *Trends Cell Biol* 19:198–206.
2. Fehon RG, McClatchey AI, Bretscher A (2010) Organizing the cell cortex: The role of ERM proteins. *Nat Rev Mol Cell Biol* 11:276–287.
3. Algrain M, Turunen O, Vaheri A, Louvard D, Arpin M (1993) Ezrin contains cytoskeleton and membrane binding domains accounting for its proposed role as a membrane-cytoskeletal linker. *J Cell Biol* 120:129–139.
4. Pearson MA, Reczek D, Bretscher A, Karplus PA (2000) Structure of the ERM protein moesin reveals the FERM domain fold masked by an extended actin binding tail domain. *Cell* 101:259–270.
5. Reczek D, Berryman M, Bretscher A (1997) Identification of EBP50: A PDZ-containing phosphoprotein that associates with members of the ezrin-radixin-moesin family. *J Cell Biol* 139:169–179.
6. Weinman EJ, Hall RA, Friedman PA, Liu-Chen LY, Shenolikar S (2006) The association of NHERF adaptor proteins with G protein-coupled receptors and receptor tyrosine kinases. *Annu Rev Physiol* 68:491–505.
7. Charras GT, Hu CK, Coughlin M, Mitchison TJ (2006) Reassembly of contractile actin cortex in cell blebs. *J Cell Biol* 175:477–490.
8. Kunda P, Pelling AE, Liu T, Baum B (2008) Moesin controls cortical rigidity, cell rounding, and spindle morphogenesis during mitosis. *Curr Biol* 18:91–101.
9. Carreno S, et al. (2008) Moesin and its activating kinase Slik are required for cortical stability and microtubule organization in mitotic cells. *J Cell Biol* 180:739–746.
10. Pilot F, Philippe JM, Lemmers C, Lecuit T (2006) Spatial control of actin organization at adherens junctions by a synaptotagmin-like protein Btsz. *Nature* 442:580–584.
11. Yonemura S, et al. (1998) Ezrin/radixin/moesin (ERM) proteins bind to a positively charged amino acid cluster in the juxta-membrane cytoplasmic domain of CD44, CD43, and ICAM-2. *J Cell Biol* 140:885–895.
12. Stanasila L, Abuin L, Diviani D, Cotecchia S (2006) Ezrin directly interacts with the alpha1b-adrenergic receptor and plays a role in receptor recycling. *J Biol Chem* 281:4354–4363.
13. Rollason R, Korolchuk V, Hamilton C, Jepson M, Banting G (2009) A CD317/tetherin-RICH2 complex plays a critical role in the organization of the subapical actin cytoskeleton in polarized epithelial cells. *J Cell Biol* 184:721–736.
14. LaLonde DP, Garbett D, Bretscher A (2010) A regulated complex of the scaffolding proteins PDZK1 and EBP50 with ezrin contribute to microvillar organization. *Mol Biol Cell* 21:1519–1529.
15. Speck O, Hughes SC, Noren NK, Kulikauskas RM, Fehon RG (2003) Moesin functions antagonistically to the Rho pathway to maintain epithelial integrity. *Nature* 421:83–87.
16. Saotome I, Curto M, McClatchey AI (2004) Ezrin is essential for epithelial organization and villus morphogenesis in the developing intestine. *Dev Cell* 6:855–864.
17. Göbel V, Barrett PL, Hall DH, Fleming JT (2004) Lumen morphogenesis in C. elegans requires the membrane-cytoskeleton linker erm-1. *Dev Cell* 6:865–873.
18. Van Fürden D, Johnson K, Segbert C, Bossinger O (2004) The C. elegans ezrin-radixin-moesin protein ERM-1 is necessary for apical junction remodelling and tubulogenesis in the intestine. *Dev Biol* 272:262–276.
19. el Marjou F, et al. (2004) Tissue-specific and inducible Cre-mediated recombination in the gut epithelium. *Genesis* 39:186–193.
20. Hughes SC, Formstecher E, Fehon RG (2010) Sip1, the Drosophila orthologue of EBP50/NHERF1, functions with the sterile 20 family kinase Slik to regulate Moesin activity. *J Cell Sci* 123:1099–1107.
21. Lamprecht G, Seidler U (2006) The emerging role of PDZ adapter proteins for regulation of intestinal ion transport. *Am J Physiol Gastrointest Liver Physiol* 291:G766–G777.
22. Bijvelds MJ, et al. (2005) Fat absorption in cystic fibrosis mice is impeded by defective lipolysis and post-lipolytic events. *Am J Physiol Gastrointest Liver Physiol* 288:G646–G653.
23. Johnson LR (2006) Apoptosis in the gastrointestinal tract. *Physiology of the Gastrointestinal Tract*, ed Johnson LR (Academic Press, New York), Vol 1, pp 345–374.
24. Rosenblatt J, Raff MC, Cramer LP (2001) An epithelial cell destined for apoptosis signals its neighbors to extrude it by an actin- and myosin-dependent mechanism. *Curr Biol* 11:1847–1857.
25. Slattum G, McGee KM, Rosenblatt J (2009) P115 RhoGEF and microtubules decide the direction apoptotic cells extrude from an epithelium. *J Cell Biol* 186:693–702.
26. Mathan M, Moxey PC, Trier JS (1976) Morphogenesis of fetal rat duodenal villi. *Am J Anat* 146:73–92.
27. Madara JL, Neutra MR, Trier JS (1981) Junctional complexes in fetal rat small intestine during morphogenesis. *Dev Biol* 86:170–178.
28. Cavey M, Rauzi M, Lenne PF, Lecuit T (2008) A two-tiered mechanism for stabilization and immobilization of E-cadherin. *Nature* 453:751–756.
29. Braga VM, Machesky LM, Hall A, Hotchin NA (1997) The small GTPases Rho and Rac are required for the establishment of cadherin-dependent cell-cell contacts. *J Cell Biol* 137:1421–1431.
30. Takaishi K, Sasaki T, Kotani H, Nishioka H, Takai Y (1997) Regulation of cell-cell adhesion by rac and rho small G proteins in MDCK cells. *J Cell Biol* 139:1047–1059.
31. Yamada S, Nelson WJ (2007) Localized zones of Rho and Rac activities drive initiation and expansion of epithelial cell-cell adhesion. *J Cell Biol* 178:517–527.
32. Yamada S, Pokutta S, Drees F, Weis WI, Nelson WJ (2005) Deconstructing the cadherin-catenin-actin complex. *Cell* 123:889–901.
33. Weis WI, Nelson WJ (2006) Re-solving the cadherin-catenin-actin conundrum. *J Biol Chem* 281:35593–35597.
34. Cavey M, Lecuit T (2009) Molecular bases of cell-cell junctions stability and dynamics. *Cold Spring Harb Perspect Biol* 1:a002998.
35. Bertet C, Sulak L, Lecuit T (2004) Myosin-dependent junction remodelling controls planar cell intercalation and axis elongation. *Nature* 429:667–671.
36. Pilot F, Lecuit T (2005) Compartmentalized morphogenesis in epithelia: From cell to tissue shape. *Dev Dyn* 232:685–694.
37. Blankenship JT, Backovic ST, Sanny JS, Weitz O, Zallen JA (2006) Multicellular rosette formation links planar cell polarity to tissue morphogenesis. *Dev Cell* 11:459–470.
38. Lecuit T, Lenne PF (2007) Cell surface mechanics and the control of cell shape, tissue patterns and morphogenesis. *Nat Rev Mol Cell Biol* 8:633–644.
39. Baena-López LA, Baonza A, García-Bellido A (2005) The orientation of cell divisions determines the shape of Drosophila organs. *Curr Biol* 15:1640–1644.
40. Fischer E, et al. (2006) Defective planar cell polarity in polycystic kidney disease. *Nat Genet* 38:21–23.
41. Gong Y, Mo C, Fraser SE (2004) Planar cell polarity signalling controls cell division orientation during zebrafish gastrulation. *Nature* 430:689–693.
42. Fleming ES, et al. (2007) Planar spindle orientation and asymmetric cytokinesis in the mouse small intestine. *J Histochem Cytochem* 55:1173–1180.
43. Quyn AJ, et al. (2010) Spindle orientation bias in gut epithelial stem cell compartments is lost in precancerous tissue. *Cell Stem Cell* 6:175–181.
44. McConnell RE, Tyska MJ (2007) Myosin-1a powers the sliding of apical membrane along microvillar actin bundles. *J Cell Biol* 177:671–681.